Proceedings of the 3rd International Conference on
Fracture Fatigue and Wear, pp. 134-140, 2014

Buckling analysis of piezoelectric composite plates using NURBS-based isogeometric finite elements and higher-order shear deformation theory

P. Phung-Van[1,2,*], M. Abdel-Wahab[2], Loc V. Tran[1] and H. Nguyen-Xuan[3]

[1]Division of Computational Mechanics, Ton Duc Thang University, Vietnam
[2]Department of Mechanical Construction and Production, Faculty of Engineering and Architecture, Ghent University, Belgium
[3]Department of Mechanics, University of Science, VNU - HCMC, Vietnam
*Corresponding author: phuc.phungvan@ugent.be

Abstract: This paper further exploits the utility and robustness of Isogeometric Analysis (IGA) together with Higher-order Shear Deformation Theory (HSDT) for buckling analysis of piezoelectric composite plates. In the composite plates, the mechanical displacement field is approximated according to the HSDT model using NURBS-based isogeometric elements. These achieve naturally any desired degree of continuity through the choice of the interpolation order, so that the method easily fulfils the C^1-continuity requirement of the HSDT model. The electric potential is assumed to vary linearly through the thickness for each piezoelectric sub-layer. The accuracy and reliability of the proposed method is verified by comparing its numerical predictions with those of other available numerical approaches.

Keywords: Isogeometric Analysis (IGA); composite plates; piezoelectricity; sensors and actuators

1 INTRODUCTION

The integration of composite plates with piezoelectric materials to obtain active lightweight smart structures has attracted a considerable interest for various applications such as automotive sensors, actuators, transducers and active damping devices. Due to the attractive properties of piezoelectric composite structures, various numerical methods have been proposed to model and simulate their behaviour. For static and free vibration analysis, Yang and Lee [1] showed that the early work on structures with piezoelectric layers could lead to substantial errors in the natural frequencies and mode shapes. Kim et al. [2] validated the Finite Element (FE) model of a smart cantilever plate through comparison with experiments. Willberg et al. [3] studied a three-dimensional piezoelectric solid model using isogeometric finite elements. For vibration control, some theories integrated with various numerical methods have been proposed and the three most popular theories are the Classical Lamination Theory (CLT), the First-order Shear Deformation Theory (FSDT), and the Higher-order Shear Deformation Theory (HSDT). In the CLT, which is based on the assumptions of Kirchhoff's plate theory, the interlaminar shear deformation is neglected. Hwang and Park [4], Lam et al. [5] reported control algorithms based on classical negative velocity feedback control and the FE method which were formulated based on the discrete Kirchhoff quadrilateral element. In the FSDT, a constant transverse shear deformation is assumed through the entire thickness of the laminate and hence stress-free boundary conditions are violated at the top and bottom surfaces of the panel. Milazzo and Orlando [6] studied free vibration analysis of smart laminated thick composite plates. Phung-Van et al. [7] extended the cell-based smoothed discrete shear gap method to static, free vibration and control of piezoelectric composite plates. In both CLT and FSDT theories, a shear correction factor is required to ensure the stability of the solution. In order to improve the accuracy of transverse shear stresses and to avoid the introduction of shear correction factors, the HSDT based on the FE method has been proposed to study piezoelectric plates [8,9]. It is worth mentioning that the HSDT requires at least C^1-continuity of generalized displacements due to the presence of their second-order derivatives in the stiffness formulation. This is a source of difficulty in standard finite elements featuring C^0 inter-element continuity. As it emerges from the above review, the available studies have focused on the dynamic analysis of piezoelectric composite plates using the FE method, the smoothed FE method, etc. This paper aims at further contributing to the dynamic analysis of piezoelectric composite plates using an

isogeometric approach based on Non-Uniform B-Spline (NURBS) basis functions. In particular, we show that a HSDT formulation fulfilling C^1-continuity requirements is easily achieved in the isogeometric framework. Isogeometric analysis (IGA) has been recently proposed by Hughes et al. [10] with the original objective to tightly integrate Computer Aided Design (CAD) and FE analysis. IGA makes use of the same basis functions typically used in the CAD environment (most notably NURBS or T-Splines) to describe the geometry of the problem exactly as it is produced from CAD as well as to approximate the solution fields for the analysis.

This paper exploits further the advantages of a NURBS-based isogeometric approach for buckling analysis of laminated composite plates integrated with piezoelectric sensors and actuators using the HSDT theory. In the composite plates, the mechanical displacement field is approximated according to the HSDT model using NURBS-based isogeometric elements. These achieve naturally any desired degree of continuity through the choice of the interpolation order, so that the method easily fulfils the C^1-continuity requirement of the HSDT model. The electric potential is assumed to vary linearly through the thickness for each piezoelectric sub-layer. The accuracy and reliability of the proposed method is verified by comparing its numerical predictions with those of other available numerical approaches.

2 WEAK FORM AND FEM FORMULATION FOR PIEZOELECTRIC COMPOSITE PLATE

2.1 Linear piezoelectric constitutive equations

The linear piezoelectric constitutive equations can be expressed as

$$\begin{bmatrix} \boldsymbol{\sigma} \\ \mathbf{D} \end{bmatrix} = \begin{bmatrix} \mathbf{c} & -\mathbf{e}^T \\ \mathbf{e} & \mathbf{g} \end{bmatrix} \begin{bmatrix} \boldsymbol{\varepsilon} \\ \mathbf{E} \end{bmatrix} \tag{1}$$

where $\boldsymbol{\sigma}$ and $\boldsymbol{\varepsilon}$ are the stress and strain vectors; **D** and **E** are dielectric displacement and electric vectors; **c** is the elasticity matrix; **e** is the piezoelectric constant matrix and **g** denotes the dielectric constant matrix.

The Galerkin weak form of the governing equations of piezoelectric structures can be derived by using Halminton's variational principle [4], which can be written as

$$L = \int \left(\tfrac{1}{2} \rho \dot{\mathbf{u}}^T \dot{\mathbf{u}} - \tfrac{1}{2} \boldsymbol{\sigma}^T \boldsymbol{\varepsilon} + \tfrac{1}{2} \mathbf{D}^T \mathbf{E} + \mathbf{u} \mathbf{f}_s - \boldsymbol{\phi} \mathbf{q}_s \right) \mathrm{d}\Omega + \sum \mathbf{u}^T \mathbf{F}_p - \sum \boldsymbol{\phi} \mathbf{Q}_p = 0 \tag{2}$$

where $\mathbf{u}$ and $\dot{\mathbf{u}}$ are the mechanical displacement and velocity; $\boldsymbol{\phi}$ is the electric potential; $\mathbf{f}_s$ and $\mathbf{F}_p$ are the mechanical loads and point loads; $\mathbf{q}_s$, $\mathbf{Q}_p$ are the surface charges and point charges.

2.2 Approximations on the mechanical displacement field

2.2.1 Governing equations for a third-order shear deformation theory model

According to the third-order shear deformation theory proposed by Reddy [11], the displacements of an arbitrary point in the plate are expressed by

$$u = u_0 + z\beta_x + cz^3 \left(\beta_x + w_{,x} \right); \; v = v_0 + z\beta_y + cz^3; \; w = w_0 \tag{3}$$

where t is the thickness of the plate; $c = 4/3t^2$ and the variables $\mathbf{u}_0 = \left[u_0 \; v_0 \right]^T$, w_0 and $\boldsymbol{\beta} = \left[\beta_x \; \beta_y \right]^T$ are the membrane displacements, the deflection of the mid-plane and the rotations of the mid-plane around y-axis and x–axis, respectively.

The strains are thus expressed by the following equation

$$\boldsymbol{\varepsilon}=\begin{bmatrix}\varepsilon_{xx}\\ \varepsilon_{yy}\\ \gamma_{xy}\end{bmatrix}=\begin{bmatrix}u_{0,x}\\ v_{0,y}\\ u_{0,y}+v_{0,x}\end{bmatrix}+z\begin{bmatrix}\beta_{x,x}\\ \beta_{y,y}\\ \beta_{x,y}+\beta_{y,x}\end{bmatrix}+z^3c\begin{bmatrix}\beta_{x,x}+w_{0,xx}\\ \beta_{y,y}+w_{0,yy}\\ \beta_{x,y}+\beta_{y,x}+2w_{0,xy}\end{bmatrix}=\boldsymbol{\varepsilon}_0+z\boldsymbol{\kappa}_1+z^3\boldsymbol{\kappa}_2 \tag{4}$$

$$\boldsymbol{\gamma}=\begin{bmatrix}\gamma_{xz}\\ \gamma_{yz}\end{bmatrix}=\begin{bmatrix}\beta_x+w_{0,x}\\ \beta_y+w_{0,y}\end{bmatrix}+z^2 3c\begin{bmatrix}\beta_x+w_{0,x}\\ \beta_y+w_{0,y}\end{bmatrix}=\boldsymbol{\varepsilon}_s+z^2\boldsymbol{\kappa}_s \tag{5}$$

From Hooke's law and the linear strains given by Eqs. (4) and (5), the stress is computed by

$$\boldsymbol{\sigma}=\begin{bmatrix}\boldsymbol{\sigma}_p\\ \boldsymbol{\tau}\end{bmatrix}=\begin{bmatrix}\overline{\mathbf{D}} & \mathbf{0}\\ \mathbf{0} & \overline{\mathbf{D}}_s\end{bmatrix}\begin{bmatrix}\boldsymbol{\varepsilon}\\ \boldsymbol{\gamma}\end{bmatrix}=\mathbf{c}\boldsymbol{\varepsilon} \tag{6}$$

where $\boldsymbol{\sigma}_p$ and $\boldsymbol{\tau}$ are the in-plane stress component and shear stress; $\overline{\mathbf{D}}$ and $\overline{\mathbf{D}}_s$ are material constant matrices given in the form of

$$\overline{\mathbf{D}}=\begin{bmatrix}\mathbf{A} & \mathbf{B} & \mathbf{E}\\ \mathbf{B} & \mathbf{D} & \mathbf{F}\\ \mathbf{E} & \mathbf{F} & \mathbf{H}\end{bmatrix},\ \overline{\mathbf{D}}_s=\begin{bmatrix}\mathbf{A}_s & \mathbf{B}_s\\ \mathbf{B}_s & \mathbf{D}_s\end{bmatrix},\ \begin{matrix}(\mathbf{A},\mathbf{B},\mathbf{D},\mathbf{E},\mathbf{F},\mathbf{H})=\int_{-h/2}^{h/2}\left(1,z,z^2,z^3,z^4,z^6\right)\overline{Q}_{ij}\mathrm{d}z\ \ (i,j=1,2,6)\\ (\mathbf{A}_s,\mathbf{B}_s,\mathbf{D}_s)=\int_{-h/2}^{h/2}\left(1,z^2,z^4\right)\overline{Q}_{ij}\mathrm{d}z\qquad i,j=4,5\end{matrix} \tag{7}$$

2.2.2 NURBS-based novel composite plate formulation

Using the NURBS basis functions [10], the displacement field **u** of the plate is approximated as

$$\mathbf{u}^h(\xi,\eta)=\sum_{I}^{m\times n}N_I(\xi,\eta)\mathbf{d}_I \tag{8}$$

where $\mathbf{d}_I=\left[u_{0I}\ \ v_{0I}\ \ w_{0I}\ \ \beta_{xI}\ \ \beta_{xI}\right]^T$ is the vector of degrees of freedom associated with the control point *I*.

Substituting Eq. (8) into Eqs. (4) and (5), the in-plane and shear strains can be rewritten as:

$$\left[\boldsymbol{\varepsilon}_0^T\ \boldsymbol{\kappa}_1^T\ \boldsymbol{\kappa}_2^T\ \boldsymbol{\varepsilon}_s^T\ \boldsymbol{\kappa}_s^T\right]^T=\sum_{A=1}^{m\times n}\left[\left(\mathbf{B}_I^m\right)^T\ \left(\mathbf{B}_I^{b1}\right)^T\ \left(\mathbf{B}_I^{b2}\right)^T\ \left(\mathbf{B}_I^{s0}\right)^T\ \left(\mathbf{B}_I^{s1}\right)^T\right]^T\mathbf{d}_I \tag{9}$$

where

$$\mathbf{B}_I^m=\begin{bmatrix}N_{I,x} & 0 & 000\\ 0 & N_{I,y} & 000\\ N_{I,y} & N_{I,x} & 000\end{bmatrix},\ \mathbf{B}_I^{b1}=\begin{bmatrix}000 & N_{I,x} & 0\\ 000 & 0 & N_{I,y}\\ 000 & N_{I,y} & N_{I,x}\end{bmatrix},\ \mathbf{B}_I^{b2}=c\begin{bmatrix}00 & N_{I,xx} & N_{I,x} & 0\\ 00 & N_{I,yy} & 0 & N_{I,y}\\ 002 & N_{I,xy} & N_{I,y} & N_{I,x}\end{bmatrix},$$
$$\mathbf{B}_I^{s0}=\begin{bmatrix}00 & N_{I,x} & N_I & 0\\ 00 & N_{I,y} & 0 & N_I\end{bmatrix},\ \mathbf{B}_I^{s1}=3c\begin{bmatrix}00 & N_{I,x} & N_I & 0\\ 00 & N_{I,y} & 0 & N_I\end{bmatrix} \tag{10}$$

2.3 Approximation of the electric potential field

In each sub-layer, a linear electric potential function is assumed through the thickness as [12]:

$$\phi^i(z) = \mathbf{N}_\phi^i \boldsymbol{\phi}^i \tag{11}$$

where $\mathbf{N}_\phi^i$ is the vector of the shape functions for the electric potential, and $\boldsymbol{\phi}^i$ is the vector containing the electric potentials at the top and bottom surfaces of the *i*-th sub-layer.

For each piezoelectric sub-layer element, the electric field **E** in Eq. (1) can be rewritten as [13]:

$$\mathbf{E} = -\nabla \mathbf{N}_\phi^i \boldsymbol{\phi}^i = -\mathbf{B}_\phi \boldsymbol{\phi}^i \tag{12}$$

2.4 Elementary governing equation of motion

The final form of equation of buckling is written in the following form

$$(\mathbf{K} - \omega^2 \mathbf{M})\mathbf{u} = 0 \quad \text{and} \quad (\mathbf{K} - \lambda_{cr} \mathbf{K}_g)\mathbf{u} = 0 \tag{13}$$

where

$$\mathbf{M} = \begin{bmatrix} \mathbf{M}_{uu} & 0 \\ 0 & 0 \end{bmatrix}, \ \mathbf{K} = \begin{bmatrix} \mathbf{K}_{uu} & \mathbf{K}_{u\phi} \\ \mathbf{K}_{\phi u} & \mathbf{K}_{\phi\phi} \end{bmatrix}, \ \mathbf{u} = \begin{bmatrix} \mathbf{d} \\ \boldsymbol{\phi} \end{bmatrix} = \begin{bmatrix} \mathbf{F} \\ \mathbf{Q} \end{bmatrix} \tag{14}$$

in which

$$\mathbf{K}_{uu} = \int_\Omega \mathbf{B}_u^T \mathbf{c} \mathbf{B}_u \mathrm{d}\Omega \ ; \ \mathbf{K}_{u\phi} = \int_\Omega \mathbf{B}_u^T \mathbf{e}^T \mathbf{B}_\phi \mathrm{d}\Omega ; \ \mathbf{K}_{\phi\phi} = -\int_\Omega \mathbf{B}_\phi^T \mathbf{p} \mathbf{B}_\phi \mathrm{d}\Omega \ ; \ \mathbf{M}_{uu} = \int_\Omega \mathbf{N}^T \mathbf{m} \mathbf{N} \mathrm{d}\Omega \tag{15}$$

which $\mathbf{B}_u = [\mathbf{B}^m \ \mathbf{B}^{b1} \ \mathbf{B}^{b2} \ \mathbf{B}^{s0} \ \mathbf{B}^{s1}]^T$; **m** is defined by

$$\mathbf{m} = \begin{bmatrix} \mathbf{I}_0 & 0 & 0 \\ 0 & \mathbf{I}_0 & 0 \\ 0 & 0 & \mathbf{I}_0 \end{bmatrix} \text{where } \mathbf{I}_0 = \begin{bmatrix} I_1 & I_2 & cI_4 \\ I_2 & I_3 & cI_5 \\ cI_4 & cI_5 & c^2 I_7 \end{bmatrix}$$
$$(I_1, I_2, I_3, I_4, I_5, I_7) = \int_{-h/2}^{h/2} \rho \left(1, z, z^2, z^3, z^4, z^7\right) \mathrm{d}z \tag{16}$$

and

$$\mathbf{K}_g = \int_\Omega \left(\mathbf{B}_g\right)^T \mathbf{N}_0 \mathbf{B}_g \mathrm{d}\Omega \quad \text{where } \mathbf{B}_g = \begin{bmatrix} 0\,0\,N_{I,x}\,0\,0 \\ 0\,0\,N_{I,y}\,0\,0 \end{bmatrix}, \ \mathbf{N}_0 \begin{bmatrix} N_x^0 & N_{xy}^0 \\ N_{xy}^0 & N_y^0 \end{bmatrix} \tag{17}$$

and ω, λ_{cr} are the natural frequency and the critical buckling value, respectively.

In this work, the constant gain G_d of the displacement feedback control is used to couple the input actuator voltage vector $\boldsymbol{\phi}_a$ and the output sensor voltage vector $\boldsymbol{\phi}_s$ as $\boldsymbol{\phi}_a = G_d \boldsymbol{\phi}_s$

The global stiffness matrix can be rewritten [7]:

$$\mathbf{K}^{*} = \mathbf{K}_{uu} + G_d \left[\mathbf{K}_{u\phi}\right]_s \left[\mathbf{K}_{\phi\phi}^{-1}\right]_s \left[\mathbf{K}_{\phi u}\right]_s \tag{18}$$

3 NUMERICAL RESULTS

In this section, first, we verify the accuracy and efficiency of the proposed isogeometric element for analyzing the natural frequencies of the piezoelectric composite plates. We consider a square five-ply piezoelectric laminated composite plate [*pie*/0/90/0/*pie*] in which *pie* denotes a piezoelectric layer. The plate is simply supported and the thickness to length ratio of each composite ply is *t/a* = 1/50. The laminate configuration includes three layers of Graphite/Epoxy (*Gp/Ep*) with fiber orientations of [0/90/0]. Two continuous PZT-4 piezoelectric layers of thickness 0.1*t* are bonded to the upper and lower surfaces of the laminate. Two sets of electric boundary conditions are considered for the inner surfaces of the piezoelectric layers including: (1) a closed-circuit condition in which the electric potential is kept zero (grounded); and (2) an open-circuit condition in which the electric potential remains free (zero electric displacements). Table 1 shows the dimensionless first natural frequency of the piezoelectric composite plate with meshing of 8×8. In this study, the isogeometric elements use the HSDT with only 5 dofs per control point while Ref [15] uses the layerwise theory and Ref [8] uses HSDT with 11 dofs per node. It is seen that the results given by the isogeometric formulation are slightly lower than the analytical solution [16], however the errors are less than 5%. We observe that the isogeometric results are stable in both a closed-circuit condition and an open-circuit condition similarly to the analytical solution [16], while those of Refs [15,8] are very different for a closed-circuit condition and an open-circuit condition.

Table 1 Dimensionless first natural frequency of the piezoelectric composite plate [*pie*/0/90/0/*pie*]

Method	Meshing	Degrees of freedom (DOFs)	$\overline{f} = \omega_1 a^2 / \left(10000 t\sqrt{\rho}\right)$	
			Closed circuit	Open circuit
IGA (5 dofs per control point)	8×8	500	235.900	236.100
FE layerwise [15]	12×12	2208	234.533	256.765
Q9 - HSDT (11 dofs per node) [8]	-	-	230.461	250.597
Q9 - FSDT (5 dofs per node) [8]	-	-	206.304	245.349
Ref [16]			245.941	245.942

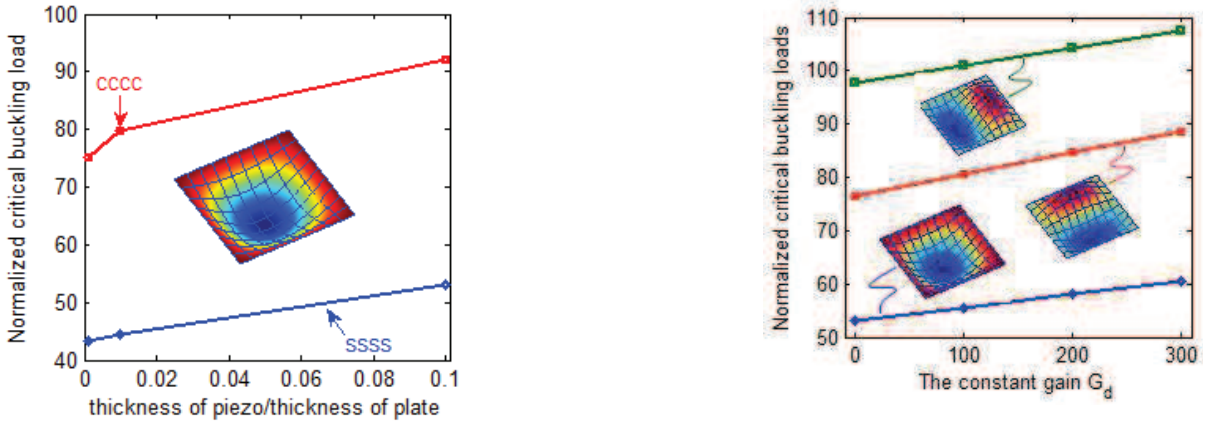

(a) The buckling loads (b) First three buckling mode

Fig. 1 Model of a 5-ply piezoelectric composite plate

Next, we consider a piezoelectric composite plate under axial compression. The buckling load parameter $\overline{\lambda}_{cr} = \lambda_{cr} a^2 / \left(10000 t \sqrt{\rho}\right)$ of piezoelectric with boundary condition: simply supported and clamped is plotted in Fig. 1a. It can be seen that the buckling load for clamped plate is higher than that for simply supported plate, as expected. This is because the stiffness of the clamped plate is stiffer. Next, the effect of the constant gain of the displacement to the buckling loads is displayed in Fig. 1b. The results show that the buckling load increases when the constraint gain increases.

4 CONCLUSIONS

This paper presents a simple and effective approach based on the combination of IGA and HSDT for the buckling analyses of composite plates integrated with piezoelectric sensors and actuators. In the piezoelectric composite plates, the mechanical displacement field is approximated according to the HSDT using isogeometric elements based on NURBS and featuring at least C^1-continuity, whereas the electric potential is assumed to vary linearly through the thickness for each piezoelectric sub-layer. The accuracy and reliability of the proposed method is verified by comparing its numerical predictions with those of other available numerical approaches.

5 REFERENCES

[1] S.M. Yang, Y.J. Lee, Interaction of structure vibration and piezoelectric actuation, Smart Materials and Structures, 3, 494–500, 1994.

[2] J. Kim, V.V. Varadan, V.K. Varadan, X.Q. Bao, Finite element modelling of a smart cantilever plate and comparison with experiments, Smart Materials and Structures, 5, 165–170, 1996.

[3] C. Willberg, U. Gabbert, Development of a three-dimensional piezoelectric isogeometric finite element for smart structure applications, Acta Mechanica, 223(8), 1837-1850, 2012.

[4] W.C. Hwang, H.C. Park, Finite element modelling of piezoelectric sensors and actuators, AIAA Journal, 31, 930-937, 1993.

[5] K.Y. Lam, X.Q. Peng, G.R. Liu, J.N. Reddy, A finite-element model for piezoelectric composite laminates, Smart Materials and Structures, 65, 83–91, 1997.

[6] A. Milazzo, C. Orlando, An equivalent single-layer approach for free vibration analysis of smart laminated thick composite plates, Smart Material and Structures, 21, 075031, 2012.

[7] P. Phung-Van, T. Nguyen-Thoi, T. Le-Dinh, H. Nguyen-Xuan, Static and free vibration analyses and dynamic control of composite plates integrated with piezoelectric sensors and actuators by the cell-based smoothed discrete shear gap method (CS-FEM-DSG3), Smart Materials and Structures, 22, 095026, 2013.

[8] M.F.C. Victor, A.A.G. Maria, S. Afzal, M.M.S. Cristóvão, A.M.S. Carlos, C.V.M. Franco, Modelling and design of adaptive composite structures, Computer Methods in Applied Mechanics and Engineering, 185, 325-346, 2000.

[9] J.N. Reddy, On laminated composite plates with integrated sensors and actuators, Engineering Structures 21, 568–593, 1999.

[10] T.J.R. Hughes, J.A. Cottrell, Y. Bazilevs, Isogeometric analysis: CAD, finite elements, NURBS, exact geometry and mesh refinement, Computer Methods in Applied Mechanics and Engineering, 194(39-41), 4135–4195, 2005.

[11] J.N. Reddy, A simple higher-order theory for laminated composite plates, Journal of Applied Mechanics, 51, 745–752, 1984.

[12] S.Y. Wang, A finite element model for the static and dynamic analysis of a piezoelectric bimorph, International Journal of Solids and Structures, 41, 4075-4096, 2004.

[13] S.Y. Wang, S.T. Quek, K.K. Ang, Vibration control of smart piezoelectric composite plates, Smart Materials and Structures, 10, 637-644, 2001.

[14] M.F.C. Victor, A.A.G. Maria, S. Afzal, M.M.S. Cristóvão, A.M.S. Carlos, C.V.M. Franco, Modelling and design of adaptive composite structures, Computer Methods in Applied Mechanics and Engineering, 185, 325-346, 2000.

[15] D.A. Saravanos, P.R. Heyliger, D.A. Hopkins, Layerwise mechanics and finite element for the dynamic analysis of piezoelectric composite plates, International Journal of Solids and Structures, 34, 359-378, 1997.

[16] P. Heyliger, D.A. Saravanos, Exact free-vibration analysis of laminated plates with embedded piezoelectric layers, Journal of the Acoustical Society of America, 98, 1547-1557, 1995.